Optical Materials 91 (2019) 195–198

Contents lists available at ScienceDirect

Optical Materials

journal homepage: www.elsevier.com/locate/optmat

Far infrared spectra of Si doped PbTe single crystals

J. Trajic[a,*], N. Paunovic[a], M. Romcevic[a], V.E. Slynko[b], Jasna L. Ristic-Djurovic[a], W.D. Dobrowolski[c], N. Romcevic[a]

[a] Institute of Physics, University of Belgrade, Pregrevica 118, 11080, Belgrade, Serbia
[b] S.P.Timoshenko Institute of Mechanics, National Academy of Sciences, Kiev, Ukraine Nesterov st., 03680, MSP, Kiev 57, Ukraine
[c] Institute of Physics, Polish Academy of Sciences, Al. Lotnikow 32/46, 02-668, Warsaw, Poland

ARTICLE INFO

Keywords:
Semiconductors
Phonons
Far-infrared spectroscopy

ABSTRACT

The far-infrared spectroscopy was used to analyze optical properties of PbTe single crystals doped with different amounts of Si. A dielectric function that takes into account the plasmon-phonon interaction was employed in the measured data manipulation. Two frequencies of plasmon-phonon coupled modes were obtained with the best-fit method, whereas the values for LO mode and plasma frequency (ω_p) were calculated. The best-fit to the experimentally obtained spectra agrees very well with the theoretical prediction.

1. Introduction

Specific physical and chemical properties of PbTe draws attention of numerous scientific studies. In particular, small band gap and high carrier mobilities qualify it for application in infrared optoelectronic devices [1] and thermoelectric materials [2]. The PbTe is also a good candidate for topological insulators materials. For instance, there are theoretical predictions that Te antisite defects in nonstoichiometric Te-rich PbTe could induce a band inversion, turning it into a topological crystalline insulator [3].

Thermoelectric materials found use in searches for alternative and complementary energy sources due to their ability to convert heat to electricity and *vice versa* [4–7]. Advantages of thermoelectric systems for direct heat-to-electricity conversion are environmental friendliness, absence of pollutants, small size, reliability, and large operating temperature range. Performance efficiency of a thermoelectric material, ZT, is expressed as $ZT = (S2\sigma/\kappa)T$, where S, T, ρ, and κ are the Seebeck coefficient, temperature, electrical resistivity, and thermal conductivity, respectively. The rocksalt-structured PbTe and related materials of n-as well as of p-type are shown to be good thermoelectric materials that operate in the mid-temperature range. As a matter of fact, PbTe-based materials have the highest recorded ZT among the bulk TE materials [8]. However, the materials based on PbTe have low mechanical strength, which can be improved by using Si as a dopant [9].

In order to absorb electromagnetic radiation, free carriers have to interact with a lattice. Transitions of an individual carrier as well as formation of collective plasma oscillators (plasmons) can contribute to the absorption. Consequently, the free-carrier absorption contains individual-carrier excitations (individual-carrier scattering), as well as collective carrier excitations (plasmon generation). Coupling of elementary excitations in solids has been investigated in a number of studies [10–13]. Studies of photon-plasmon processes usually start with a dielectric function for free carriers in a perfect crystal. Our approach [14,15] is to create a dielectric function that explains registered processes, and to compare it to the parameters obtained with the classical approach [13,16,17]. Comparison of the two yields to the physical explanation of the processes that take place in the doped semiconductors.

Raman spectroscopy is the commonly used technique to analyze optical properties of different materials. But, acquiring information about the coupled plasmon-phonon modes from the Raman spectra of PbTe samples is closely related to the ability to eliminate the influence of the oxide layer that is being formed at the sample surface. For film-samples, an additional problem can be removal of the substrate influence [18]. Further, analysis of the obtained results must be performed with elaborate mechanisms related to the microscopic approach in calculation of the Raman scattering cross-section [11] because the position of plasmon-phonon modes does not always coincide with the spectral maximum. Use of the IR spectroscopy in the analysis of the coupled plasmon-phonon modes takes into account all of these issues. In addition, in IR spectroscopy the position of global minimum remains directly related to the frequency of the coupled plasmon-phonon modes.

In this paper far-infrared spectroscopy (FIR) is used to study optical properties of PbTe single crystals doped with Si. Three values of Si

* Corresponding author.
E-mail address: jelena@ipb.ac.rs (J. Trajic).

https://doi.org/10.1016/j.optmat.2019.03.026
Received 12 February 2019; Received in revised form 7 March 2019; Accepted 18 March 2019
Available online 25 March 2019

concentration in the samples were considered, namely 1, 3, 5.6 at.%. Analysis of the reflection spectra in a wide spectral range was used to detect plasmon-phonon coupling in the studied system.

2. Experiment

Single crystal ingots of PbTe(Si) were grown by the modified Bridgman method. The samples were synthesized using high purity components. The impurity content in the starting mixture was from 3 to 8 at.%. The Si concentration in the crystals used here was 1, 3, and 5.6 at.%. Distribution of silicon along ingots was determined by the XRF (X-ray fluorescence) analysis. Prior to analysis, the ingots were cut into discs of the same thicknesses. The XRF measurements were carried out on both sides of each disc and the spectra are given as the average of the two. Distribution of silicon along these ingots is in accordance with the model given in Ref. [19] according to which impurities always moves back to the end of the ingot.

The infrared reflectivity measurements were carried out at room temperature with a BOMEM DA-8 Fourier-transform IR spectrometer. A deuterated triglycine sulfate (DTGS) pyroelectric detector was used to cover the wave number region from 50 to 450 cm^{-1}.

3. Results and discussion

The low-frequency dielectric properties of single crystals are described by classical oscillators corresponding to the TO-modes and the Drude part which takes into account the free carrier contribution [10,17]:

$$\varepsilon_S(\omega) = \varepsilon_\infty + \sum_{k=1}^{n} \frac{\varepsilon_\infty(\omega_{LOk}^2 - \omega_{TOk}^2)}{\omega_{TOk}^2 - \omega^2 - i\gamma_{TOk}\omega} - \frac{\varepsilon_\infty\omega_P^2}{\omega(\omega + i\gamma_P)} \quad (1)$$

where ε_∞, ω_{LOk}, ω_{TOk}, ω_P, γ_{TOk}, and γ_P are the bound charge contribution taken to be constant, longitudinal and transverse optical-phonon frequencies, plasma frequency, and phonon and plasma damping. Therefore, the TO mode frequency is obtained directly from the fit, whereas the LO modes are determined from the maximum of the dielectric loss function.

In the PbTe doped with Si the pure LO-mode of the lattice is strongly influenced by the plasmon mode of the free carriers, which causes appearance of a combined plasmon-LO phonon mode [12]. Consequently, only coupled mode positions are observable in the experimental spectra and the LO-modes are detectable only if the influence of the free carrier is eliminated [13]. Therefore, in the analysis of far-infrared reflectivity spectra of PbTe doped with Si we used the dielectric function that includes the interaction between LO phonon and a plasmon, i.e. the plasmon-phonon interaction in its initial form [13, 15]. Namely, the expression for dielectric function is

$$\varepsilon_f(\omega) = \varepsilon_\infty \frac{\prod_{j=1}^{2}(\omega^2 + i\gamma_{lj}\omega - \omega_{lj}^2)}{\omega(\omega + i\gamma_P)(\omega^2 + i\gamma_t\omega - \omega_t^2)} \cdot \prod_{p=1}^{l} \frac{\omega^2 + i\gamma_{LOp}\omega - \omega_{LOp}^2}{\omega^2 + i\gamma_{TOp}\omega - \omega_{TOp}^2} \quad (2)$$

The parameters ω_{lj} and γ_{lj} in the first numerator represent the eigenfrequencies and damping coefficients of the coupled plasmon-longitudinal phonon waves. The parameters in the first denominator correspond to the similar characteristics of the transverse (TO) vibrations. The second term in Eq. (2) represents l uncoupled modes of the crystal. Consequently, ω_{LOp} and ω_{TOp} are the longitudinal and transverse frequencies, whereas γ_{LOp} and γ_{TOp} are the corresponding damping parameters. Therefore, the determination of LO-mode and plasma frequency is connected with the decoupled procedure.

The far-infrared reflection spectrum at room temperature of the PbTe single crystal doped with 1 at.% Si is presented in Fig. 1. The experimental data are depicted with circles, whereas the solid line represents the calculated reflectivity spectrum, which is obtained by the fitting procedure that is based on the model for plasmon-phonon coupling given by Eq. (2). In the fitting procedure, the modes characteristic

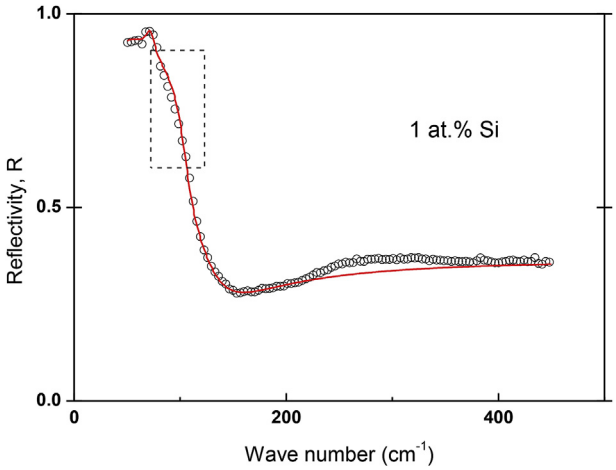

Fig. 1. Far-infrared reflection spectra of PbTe single crystal doped with 1 at.% Si. The spectrum obtained experimentally at room temperature is presented with circles. The solid lines depict the calculated spectrum obtained by the fitting procedure that is based on the model given by Eq. (2) where $p = 1$.

for this type of material are included, namely the pair of PbTe TO/LO modes and the mode at about 73 cm^{-1}, which is the PbTe Brillouin zone edge mode. These modes are considered because the phonon density of PbTe has a maximum at their frequencies [20].

Slight discrepancy between the theoretical spectrum and the experimental results in the frequency range at about 100 cm^{-1} (marked by dashed lines) indicates the existence of the mode that corresponds to the Si impurity. Fig. 2 shows the same spectrum as Fig. 1; however, in addition to the modes considered previously, the fitting procedure contains the Si impurity mode at about 90 cm^{-1}. Note that lead telluride grows with rather high concentration of native defects (vacancies, etc). In the PbTe lattice Si is a substitute for Pb and as such is a substitution impurity ion. Consequently, every ion in PbTe is no longer in the center of inversion symmetry and PbTe vibration modes could be Raman as well as far-infrared active. The impurity mode can arise simply because of the difference between masses and force constants of the impurity ion and the ion of the host material [21]. Their appearance can be caused by more complex mechanism of electron-phonon interaction [22]. When the semiconductor is doped with a substitution impurity [10] (in our case Si), and if the substitution takes place with the atoms of the heavier mass (Pb), lighter impurity leads to two modes: a

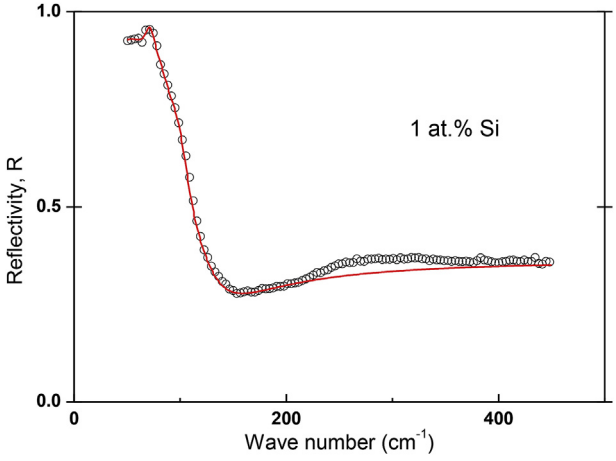

Fig. 2. Far-infrared reflection spectra of PbTe single crystal doped with 1 at.% Si. The experimental spectrum obtained at room temperature is presented with circles. The solid lines are calculated spectrum with additional Si impurity mode, obtained by the fitting procedure that is based on the model given by Eq. (2) where $p = 2$.

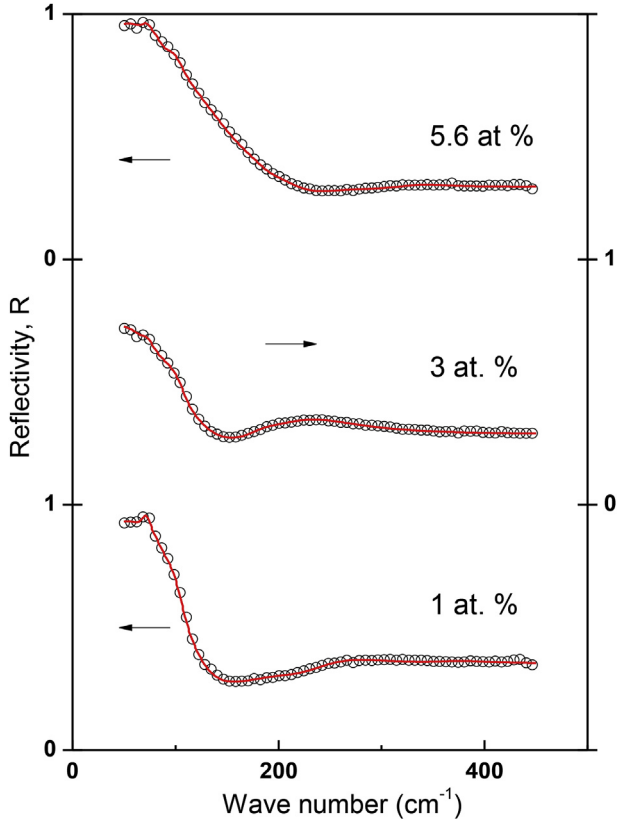

Fig. 3. Far-infrared reflection spectra of PbTe single crystals doped with 1, 3 and 5.6 at.% Si. The experimental spectra obtained at room temperature are depicted with circles. The solid lines are calculated spectra obtained by the fitting procedure that is based on the model given by Eqs. (2) and (4).

local mode situated above the optical band and a gap mode situated above the acoustic band and below the optical band of the host lattice. The position of Si impurity mode in PbTe was estimated in the manner described in detail in Ref. [23], namely with the expression

$$\omega_I(Si) = \omega_{TO}(PbTe)\sqrt{\frac{M_{Pb}}{M_{Si}}} \tag{3}$$

where M_{Pb} and M_{Si} are the masses of the atoms Pb and Si, respectively.

We did not manage to determine the set of parameters that provide good spectrum overlapping in the whole range of frequencies. Registered discrepancy between the experimental and the calculated reflectivity spectra is obvious, and the new structure is observable above 220 cm^{-1} In order to remove this discrepancy, Eqs. (1) and (2) were extended to include the term [24]:

$$\frac{\omega_{loc}^2}{\omega_0^2 - \omega^2 - i\omega G} \tag{4}$$

where ω_0, G, and ω_{loc} are the characteristic frequency, damping, and "strength" of the additional oscillator. According to Ref. [24], $(\omega_{loc})^2$ is proportional to the N_{loc} carrier concentration at the localized level.

In Fig. 3 we compare the experimental results to the theoretical spectrum at room temperature of PbTe single crystals doped with 1, 3 and 5.6 at.% Si, which take into account additional term described with Eq. (4) in Eq. (2).

We obtained the value of $\omega_0 = 235 \pm 8\,cm^{-1}$ as the result of the best fit procedure. In the SiTe electron transition from the excited state E to the ground state X exists in the range above 220 cm^{-1} [25]. It seems that during the process of doping PbTe with Si, localization of electrons occurs in the vicinity of Si impurity atom as a consequence of the appearance of Te−SiTe clusters with cubic symmetry. As one can see from Fig. 4, the "strength" of the oscillator connected with electron transition increases with the increase of Si concentration.

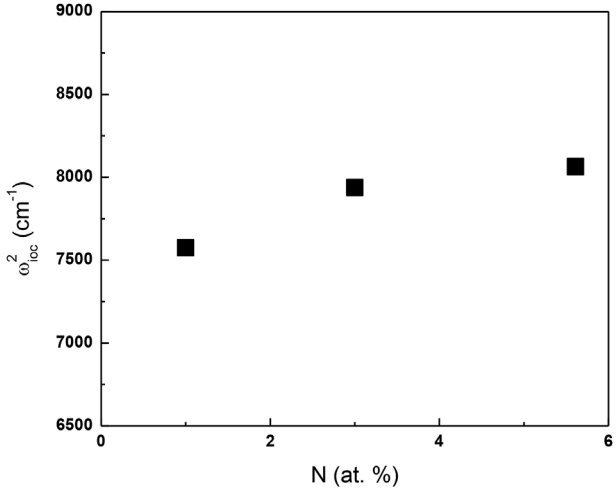

Fig. 4. The "strength" of the oscillator described by Eq. (4) vs silicon concentration.

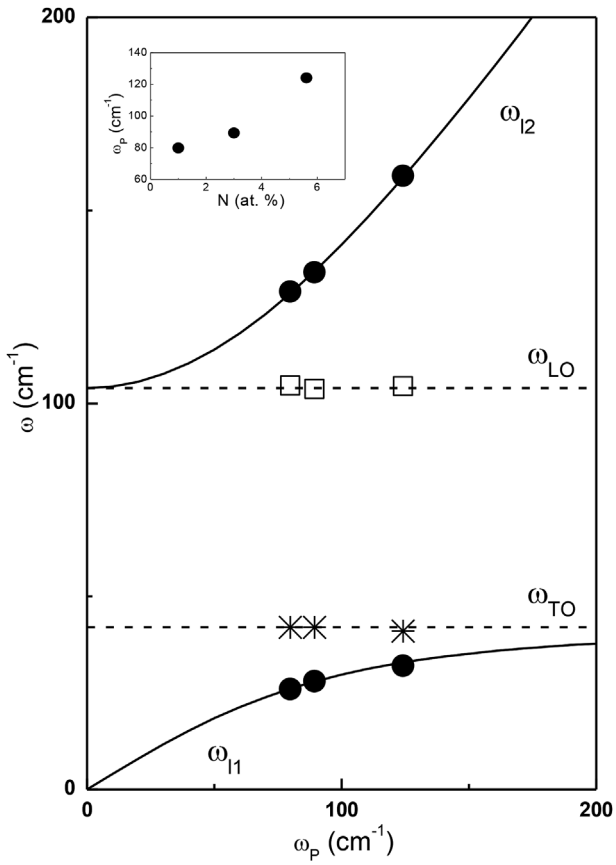

Fig. 5. The eigenfrequencies of the plasmon-LO phonon modes (full lines - Eq. (1)); ● - eigenfrequency spectra ω_{lj} obtained by procedure based on Eq. (2); □ - calculated values for ω_{LO} and * - experimentally determined values for ωTO. Inset: plasma frequencies (ω_P) vs. Si concentration.

In Fig. 5 characteristic spectra for plasmon-phonon interaction are presented. Obtained results describe the relationship between the results obtained with Eq. (2) and those resulting from the traditional approach described with Eq. (1). The solid lines represent coupled frequencies, and as it was given in Ref. [13], the positions of the coupled modes were defined as the solutions of Eq. (1) (Re{ε} = 0). Dashed

lines, obtained experimentally as the best fit, correspond to the well-known values for PbTe LO and TO phonon positions [19]. As a result of the best fit, using Eq. (2) with additional term given by Eq. (4), we obtained the frequencies of coupled modes (ω_{l1} and ω_{l2}), and then we calculated the values for ω_{LOPbTe} and ω_P, as is described in Ref. [15]. The value for the ω_{LOPbTe} obtained in this manner is in good agreement with the literature. The characteristic parameters obtained as the best fit are shown in Fig. 5. The plasma frequencies (ωP) dependence on Si concentration is presented in the inset of Fig. 5.

As we already said, localization of electrons occurs in the vicinity of the impurity, i.e. Si atom. Localization of electrons leads to the decrease of electrical conductivity. Since the thermal and electrical conductivities are proportional (Wiedemann-Franz Law), the decrease of electrical conductivity causes the decrease of thermal conductivity. Also, electrons localized around this impurity cause the localization of phonons. Since phonons are responsible for heat transmission, their localization also leads to the decrease of phonon thermal conductivity. As it is well known, a good thermoelectric material must have low thermal conductivity in order to retain the heat and to reduce the heat transfer losses. This lead us to conclude that localization of electrons in the vicinity of Si atom impurity makes PbTe doped with Si a good thermoelectric material.

These results are very significant since they represent the basis for investigation these effects in nanocrystals [26].

4. Conclusion

The far-infrared spectroscopy was employed to investigate phonon properties of PbTe single crystal doped by 1, 3, and 5.6 at.% Si. The spectra were analyzed using the dielectric function that takes into account the existence of plasmon-phonon interaction in advance. As a result of the best fit procedure the two frequencies corresponding to the coupled modes (ω_{l1} and ω_{l2}) were obtained, whereas the frequency values for LO mode (ω_{LO}) and plasma frequency (ω_P) were calculated. In addition to the modes that are characteristic for this type of material, we registered the Si impurity mode as well as the localization of electrons in the vicinity of Si impurity atom.

Declaration of interests

The authors declare that they have no known competing financial interests or personal relationships that could have appeared to influence the work reported in this paper.

Acknowledgements

This work was supported under the Agreement of Scientific Collaboration between Polish Academy of Science and Serbian Academy of Sciences and Arts. This research was financially supported by the Serbian Ministry of Education, Science and Technological Development (Project 45003).

References

[1] A.M. Samylov, M.K. Saharov, S.A. Buchnev, A.M. Khoviev, E.A. Dolgopolova, Crystal structure, carrier concentration and IR-sensitivity of PbTe thin films doped with Ga by two different methods, J. Cryst. Growth 240 (3) (2002) 340–346.
[2] M.S. Dresselhaus, G. Dresselhaus, X. Sun, Z. Zhang, S. Cronin, T. Koda, Y.I. Ying, The promise of low-dimensional thermoelectric materials, Microscale Thermophys. Eng. 3 (2) (1999) 89–100.
[3] M. Songsong, G. Chunyu, X. Chengcheng, W. Fan, S. Michael, L. Yunhao, Y. Huiqiu, W. Huizhen, Adv. Funct. Mater. 28 (2018) 1803188.
[4] X. Shi, L. Chen, C. Uher, Recent advances in high-performance bulk thermoelectric materials, Int. Mater. Rev. 61 (6) (2016) 379–415.
[5] G. Tan, L.D. Zhao, M.G. Kanatzidis, Rationally designing high-performance bulk thermoelectric materials, Chem. Rev. 116 (19) (2016) 12123–12149.
[6] J. He, T.M. Tritt, Advances in thermoelectric materials research: looking back and moving forward, Science 357 (2017) 1369.
[7] L. Yang, Z.G. Chen, M.S. Dargusch, High performance thermoelectric materials: progress and their applications, Adv. Energy Mater. 8 (6) (2017) 1701797.
[8] B. Cai, J. Li, H. Sun, L. Zhang, B. Xu, W. Hu, D. Yu, J. He, Z. Zhao, Z. Liu, Y. Tian, Enhanced thermoelectric performance of Na-doped PbTe synthesized under high pressure, Sci. China Mater. 61 (9) (2018) 1218–1224.
[9] Q. Zhang, H. Wang, Q. Zhang, W. Liu, B. Yu, H. Wang, D. Wang, G. Ni, G. Chen, Z. Ren, Effect of silicon and sodium on thermoelectric properties of thallium-doped lead telluride-based materials, Nano Lett. 12 (5) (2012) 2324–2330.
[10] E. Burstein, A. Pinczuk, R.F. Wallis, By D.L. Carter, R.T. Bate (Eds.), The Physics of Semimetals and Narrow-Gap Semiconductors, Pergamon, New York, 1971, p. 251.
[11] M. Cardona, G. Gunterodt (Eds.), Light Scattering in Solids, Top. Appl. Phys. vol. 8, Springer, Berlin, 1975.
[12] S. Takaoka, T. Hamaguchi, S. Shimomura, K. Murase, Observation of the coupled plasmon-lo phonon mode energy in photo-excited Pb1-xSnxTe doped with indium impurities, Solid State Commun. 54 (1) (1985) 99–102.
[13] A.A. Kuharskii, Solid State Commun. 8 (1970) 1275.
[14] J. Trajic, N. Romcevic, M. Romcevic, D. Stojanovic, R. Rudolf, T.A. Kuznetsova, D.R. Khokhlov, Far-infrared study of impurity local modes in Co-doped PbTe, J. Alloy. Comp. 493 (1–2) (2010) 41–46.
[15] J. Trajić, N. Romčević, M. Romčević, V.N. Nikiforov, Plasmon-phonon and plasmon-two different phonon interaction in Pb1-xMnxTe mixed crystals, Mater. Res. Bull. 42 (12) (2007) 2192–2201.
[16] V. Gopal, Analysis of the infrared plasma reflectivity spectra of semiconductors, Infrared Phys. 18 (2) (1978) 121–125.
[17] G. Abstreiter, M. Cardona, A. Pinczuk, M. Cardona, G. Guntherodt (Eds.), Light Scattering in Solids, IV, Springer-Verlag, Berlin, 1984.
[18] H. Wu, C. Cao, J. Si, T. Xu, H. Zhang, H. Wu, J. Chen, W. Shen, N. Dai, Observation of phonon modes in epitaxial PbTe films grown by molecular beam epitaxy, J. Appl. Phys. 101 (10) (2007) 103505.
[19] B.A. Volkov, L.I. Ryabova, D.R. Khokhlov, Mixed-valence impurities in lead telluride-based solid solutions, Uspekhi Fizicheskih Nauk 172 (8) (2002) 875–906 [Phys. Usp. 45 (8) (2002) pp. 819–846].
[20] W. Cochran, R.A. Cowley, G. Dolling, M.M. Elcombe, The crystal dynamics of lead telluride, Proc. R. Soc. A 293 (1966) 433–451.
[21] A.A. Maradudin, F. Seitz, D. Turnball (Eds.), Solid State Physics, vol. 19, Academic, New York, 1966.
[22] D.E. McCumber, One-phonon collision corrections to the high-frequency dielectric function of semiconductors, Phys. Rev. 154 (1967) 790.
[23] S. Venigopalan, A. Petrov, R.R. Galazka, A.K. Ramdas, S. Rodriguez, Raman scattering by phonons and magnons in semimagnetic semiconductors: Cd1 − xMnxTe, Phys. Rev. B 25 (1982) 2681.
[24] N. Romcevic, Z.V. Popovic, D. Khokhliv, A.V. Nikorich, V. Konig, Far-infrared study of localized states in In-doped Pb0. 75Sn0.25Te single crystals, Phys. Rev. B 43 (8) (1991) 6712–6716.
[25] S. Chattopadhyaya, A. Pramanik, A. Banerjee, K. Kumar Das, Electronic states and spectroscopic properties of SiTe and $SiTe^+$, J. Phys. Chem. A 110 (44) (2006) 12303–12311.
[26] J. Mitric, N. Paunovic, M. Mitric, B. Vasic, U. Ralevic, J. Trajic, M. Romcevic, W.D. Dobrowolski, I.S. Yahia, N. Romcevic, Surface optical phonon – plasmon interaction in nanodimensional CdTe thin films, Phys. E Low-dimens. Syst. Nanostruct. 104 (2018) 64–70.